Published OnlineFirst July 14, 2010; DOI: 10.1158/0008-5472.CAN-09-4008

Cancer Research

FOXO3 Encodes a Carcinogen-Activated Transcription Factor Frequently Deleted in Early-Stage Lung Adenocarcinoma

Oliver R. Mikse[1], Daniel C. Blake, Jr.[1], Nathan R. Jones[1], Yuan-Wan Sun[2], Shantu Amin[1], Carla J. Gallagher[3], Philip Lazarus[1], Judith Weisz[4], and Christopher R. Herzog[1]

Abstract

The FOXO family of transcription factors elicits cell cycle arrest, apoptosis, and resistance to various physiologic and pathologic stresses relevant to sporadic cancer, such as DNA damage and oxidative stress. Although implicated as tumor suppressors, FOXO genetic inactivation has not been observed in human cancer. In an investigation of the two major types of non–small cell lung cancer, here, we identify the *FOXO3* gene as a novel target of deletion in human lung adenocarcinoma (LAC). Biallelic or homozygous deletion (HD) of *FOXO3* was detected in 8 of 33 (24.2%) mostly early-stage LAC of smokers. Another 60.6% of these tumors had losses of *FOXO3* not reaching the level of HD (hereafter referred to as sub-HD). In contrast, no HD of *FOXO3* was observed in 19 lung squamous cell carcinoma. Consistent with the deletion of *FOXO3* were corresponding decreases in its mRNA and protein levels in LAC. The potential role of FOXO3 loss in LAC was also investigated. The carcinogen (+)-anti-7,8-dihydroxy-9,10-epoxy-7,8,9,10-tetrahydrobenzo[a]pyrene (BPDE) is strongly implicated as a cause of human lung cancer. Here, we show that FOXO3a is functionally activated and augments the level of caspase-dependent apoptosis in cells exposed to this DNA-damaging carcinogen. These results implicate FOXO3 as a suppressor of LAC carcinogenesis, a role frequently lost through gene deletion. *Cancer Res; 70(15); 6205–15. ©2010 AACR.*

Introduction

Lung cancer exceeds all cancer types as the leading cause of cancer death worldwide (1). Eighty-seven percent of these cases are classified as non–small cell lung cancer (NSCLC), among which lung adenocarcinoma (LAC) and lung squamous cell carcinoma (LSqCC) are major histotypes (1). The majority of lung cancer is causally linked to chronic exposure to air-borne carcinogens (2–4). In particular, epidemiologic and experimental studies together have established that carcinogens present in cigarette smoke account for ~85% of all human lung cancer (2–4).

LAC and LSqCC develop through distinct pathogenetic pathways, and they respond differently to treatment (5, 6). Another level of complexity to the underlying biology of these tumors is that those of smokers and never smokers also have some distinct molecular and clinical characteristics and as such can be viewed as separate diseases (7). Compared with LACs, LSqCCs tend to have higher incidences of *TP53* inactivation and allelic losses on chromosomes 13q14 (*RB*), 9p21 (*p16INK4a*), 8p21-23, and several regions of 3p (reviewed in refs. 5, 6). In LAC, mutations of *K-ras, epidermal growth factor receptor* (*EGFR*), and *Her2/neu* and allelic losses on 6q and 19p are more typical (8–12). Comprehensive genome-wide studies have also revealed many unidentified genes that are recurrently altered in and, therefore, are likely to contribute in some way to the development of these tumor types (13–15). The identification and characterization of these unknown participants should further our understanding of NSCLC and, ultimately, lead to improved therapies.

Functions that contribute to the inhibition or suppression of cancer are often selectively inactivated in tumors by gene deletion. This can occur as a consequence of any of several errors in chromosome maintenance, such as mitotic recombination, mitotic nondisjunction, chromosomal breakage, or rearrangement (16–19). Quantitative PCR (qPCR) is a validated tool to quantify the relative copy number of specific DNA sequences that result from these defects (20–23). With the availability of highly dense databases of the annotated human and mouse genomes, PCR now essentially has single-nucleotide resolution for detecting genetic targets of copy number changes. We recently showed by qPCR that *FOXO3* is deleted in carcinogen-induced LAC of mice and in human NSCLC cell lines (24, 25). This suggests that FOXO3 loss contributes to NSCLC pathogenesis.

The proposition that FOXO3 is a "tumor suppressor" is supported by several lines of evidence. FOXO3 is one of four related FOXO transcription factors that protect cells against

Authors' Affiliations: Departments of [1]Pharmacology, [2]Biochemistry and Molecular Biology, [3]Public Health Sciences, and [4]Obstetrics and Gynecology, Pennsylvania State University College of Medicine, Hershey, Pennsylvania

Note: Supplementary data for this article are available at Cancer Research Online (http://cancerres.aacrjournals.org/).

Corresponding Author: Christopher R. Herzog, Department of Pharmacology, Pennsylvania State University College of Medicine, Hershey, PA 17033. Phone: 717-531-5986; Fax: 717-531-5031; E-mail: crh13@psu.edu.

doi: 10.1158/0008-5472.CAN-09-4008

Published OnlineFirst July 14, 2010; DOI: 10.1158/0008-5472.CAN-09-4008

a wide range of physiologic stresses (26). In particular, FOXO3 has been shown to play a role in DNA repair, growth arrest, and apoptosis in response to DNA damage and oxidative stress (26–29). We recently showed that FOXO3 activates a proapoptotic transcription program and cellular response to the human lung carcinogen 4-(methylnitrosamino)-I-(3-pyridyl)-1-butanone (NNK; ref. 25). FOXOs are negatively regulated at the protein level by the serine/threonine kinase, Akt (26, 31–33). Akt phosphorylates FOXOs on specific residues that promote 14-3-3 binding and results in its cytosolic retention and transcriptional inactivation (31–33). Akt is activated by EGFR–phosphatidylinositol 3-kinase (PI3K) signaling, a pathway frequently upregulated in NSCLC (5, 10). Under certain stress conditions, the negative control of FOXOs by Akt is overcome through both phosphorylation and acetylation of FOXOs, which results in their transcriptional activation (reviewed in refs. 26, 34). Finally, the tumor suppressor roles of FOXOs have been confirmed in mice, where it was shown that germline inactivation of *Foxo1, Foxo3*, and *Foxo4* (*Foxo6* was not examined) predisposed mice to lineage-specific tumorigenesis (35). Here, we show that *FOXO3* is selectively deleted in human LAC. We also show that FOXO3 is functionally activated by and elicits a proapoptotic response to (+)-anti-7,8-dihydroxy-9,10-epoxy-7,8,9,10-tetrahydrobenzo[a]pyrene (BPDE), a human lung carcinogen. The findings of this study implicate FOXO3 as an anticarcinogenic suppressor of LAC.

Materials and Methods

Tissues and cell lines

Human lung tissues were obtained from the tumor and tissue bank of the Penn State Cancer Institute (Institutional Review Board protocols 24072EP and 29448EP). Tumor stage was assigned using standard tumor-node-metastasis criteria. Normal lung tissue was obtained from the Sun Health Research Institute's Brain and Body Donation Program for which the autopsy results showed normal lungs. Samples were excluded for any type of abnormality, including gross and microscopic abnormalities such as bronchopneumonia, lung cancer, or metastatic cancer. The majority of the tumors, both LAC and LSqCC, examined in this study were early-stage carcinoma (see Fig. 1D for the stage of each of the tumors examined in this study). Genomic DNA was isolated from frozen patient samples using previously published methods (20). H358, A549, and H1299 cell lines were obtained from the American Type Culture Collection. All cell lines were grown in RPMI 1640 supplemented with 10% fetal bovine serum, 2 mmol/L glutamine, 100 μg/mL penicillin, and 100 mg/mL streptomycin in a humidified incubator at 37°C, 20% O_2, and 5% CO_2.

Deletion analysis

Gene deletions were determined by qPCR of genomic DNA, as previously reported (20, 24). PCR was carried out as follows: 95°C for 2 minutes followed by 22 to 25 cycles (i.e., within exponential phase) at 95°C, 55°C to 60°C, and 72°C each for 30 seconds. PCR products were resolved in 2% agarose gels stained with ethidium bromide. Deletions were determined by calculating target intensity/control intensity in the tumors and cell lines divided by that value obtained from normal DNA. *Glyceraldehyde-3-phosphate dehydrogenase* (*GAPDH*) and *β-ACTIN* were used as controls. Several primer pairs were used in the deletion analysis of *FOXO3* and its flanking genes, *ARMC2* and *LACE1*. Primers for FOXO3 used in this study are listed in Table 1. Additional primer pairs used include (5′-3′) ARMC2-1 (forward, ATACACTCTGCGAACTGAAGGGGTGCT; reverse, TGCTGAGCTTCTGTTTCCTCCGAT), LACE1-1 (forward, GTGTCAAATTCCAGCCAACAGGCA; reverse, TGCTGCAAGGAGAGCAAGTGTCTA), β-ACTIN (forward, GCACCACACCTTCTACAATGAG; reverse, CTTCATGAGGTAGTCAGTCAGG), GAPDH (forward, GTATTGGGCGCCTGGTCACC; reverse, CAGTGGACTCCACGACGTAC), FOXO1 (forward, TATGAACCGCCTGACCCAAGTGAA; reverse, TCGTTGTCTTGACACTGTGTGGGA), and FOXO4 (forward, AGTTCAAATGCCAGCAGTGTCAGC; reverse, TGCTGCAAAGAGAAGCCAGAGAGA). Primers used were designed based on the available gene sequences from National Center for Biotechnology Information (NCBI) and Ensembl genome browsers and purchased from Integrated DNA Technologies. Oligos were designed to avoid known single-nucleotide polymorphisms that may affect gene dose quantitation.

Quantification was carried out by densitometry using UVP Imaging and Analysis System and LabWorks software (UVP, Inc.). Gene dose was quantified as follows: test gene intensity/control gene intensity of tumor DNA divided by that of normal (noncancerous) tissue DNA as previously described (24). To account for genetic and cellular heterogeneity of the tumor samples, gene homozygous deletion (HD) was defined as a reproducible gene dose reduction of ≥80% relative to normal DNA. A gene reduction of 40% to 80% relative to control levels was considered a hemizygous or subclonal homozygous loss. For deletion scoring, a minimum of two contiguous, nonoverlapping PCR products within *FOXO3* must have met the threshold of HD or sub-HD. The approximate locations of the *FOXO3* primers used are shown in Table 1 and Fig. 1B.

Mutation analysis

Examination of tumors and cell lines for mutations within the coding region of human *FOXO3* (i.e., exons 2 and 3) was carried out by direct sequence analysis of PCR-amplified fragments. Sequencing was performed by the Genomics Core Facility of the Penn State University using an ABI Hitachi 3730XL DNA Analyzer using protocols provided by the manufacturer.

RNA extraction and cDNA synthesis

Total RNA was extracted from tissue samples using RNeasy Mini kit (Qiagen) according to the manufacturer's protocol. Samples were subjected to on-column DNase I digestion during extraction to prevent confounding of the results by genomic DNA contamination. RNA concentrations were determined using a NanoDrop ND-1000 spectrophotometer, and RNA purity was assessed by absorbance ratios

Published OnlineFirst July 14, 2010; DOI: 10.1158/0008-5472.CAN-09-4008

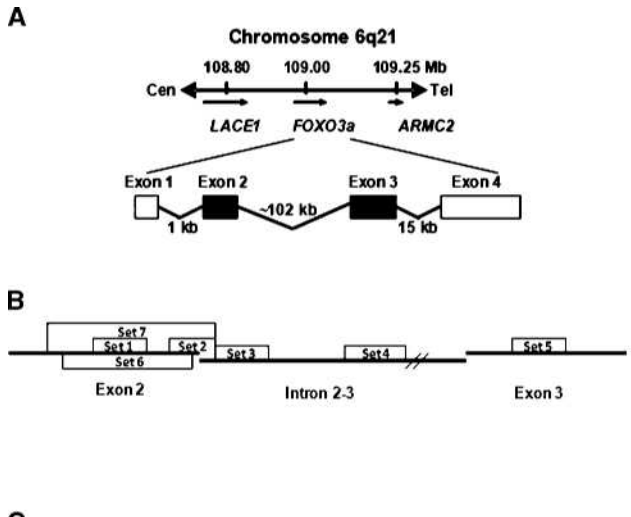

D

				FOXO3a					
ID	Tumor	Stage	LACE1	Set 1	Set 2	Set 3	Set 4	Set 5	ARMC2
Normal			1.00	1.00	1.00	1.00	1.00	1.00	1.00
6014	AC	1A	0.46	0.18	0.14	0.14	0.24	0.55	0.69
321	AC	1A	ND	0.22	0.22	0.23	0.24	0.84	ND
6765	AC	1A	0.44	0.23	0.29	0.60	0.25	0.62	0.80
2924	AC	1A	0.32	0.35	0.16	0.16	0.15	0.61	0.55
6204	AC	1A	0.60	0.46	0.31	0.59	0.41	0.46	0.48
6986	AC	1B	0.47	0.15	0.14	0.13	0.09	0.76	0.53
362	AC	1B	0.34	0.23	0.24	0.26	0.17	0.55	0.29
6498	AC	1B	0.38	0.16	0.11	0.16	0.23	0.62	0.24
6379	AC	1B	0.35	0.15	0.20	0.16	0.14	0.52	0.31
368	AC	1B	0.55	0.46	0.45	0.48	ND	0.77	0.66
6784	AC	1B	1.01	0.64	0.83	0.83	1.12	0.76	0.44
2710	AC	1B	0.39	0.46	0.49	0.38	1.32	0.81	1.10
2346	AC	1B	0.43	0.32	0.32	0.37	0.39	0.59	0.49
6040	AC	1B	0.60	0.36	0.57	0.69	0.58	0.71	1.43
308	AC	1B	ND	0.28	0.27	0.41	ND	1.13	ND
4458	AC	1B	ND	1.21	0.83	ND	0.90	1.75	ND
319	AC	1	ND	0.15	0.13	0.22	ND	1.01	ND
4891	AC	1	ND	0.28	0.52	0.44	ND	0.75	ND
6893	AC	1	0.74	0.07	0.14	0.09	0.10	0.54	0.88
2621	AC	2A	1.11	0.45	0.44	0.50	0.56	0.73	0.59
2138	AC	2A	0.35	0.36	0.25	0.26	0.32	0.50	0.65
2949	AC	2B	0.51	0.56	0.48	0.45	0.29	0.77	0.79
2742	AC	2B	0.52	0.42	0.41	0.67	0.47	0.75	0.52
359	AC	2B	ND	0.55	0.30	0.34	0.41	0.74	ND
364	AC	3A	ND	1.20	1.04	1.01	ND	0.66	ND
6095	AC	3B	0.26	0.46	0.35	0.46	0.21	0.49	0.73
4137	AC	3	ND	1.16	ND	ND	ND	ND	ND
6483	AC	4	ND	ND	ND	0.41	ND	ND	0.74
2091	AC	4	0.44	0.13	0.14	0.13	0.15	0.77	ND
357	AC	4	ND	0.21	0.25	0.22	ND	1.03	ND
318	AC	4	ND	0.23	0.24	0.22	0.42	0.59	ND
350	AC	NA	ND	0.26	0.39	0.36	ND	1.12	ND
4469	AC	NA	ND	ND	1.14	0.94	0.69	ND	ND
6399	SqCC	1A	0.62	1.01	0.99	0.99	ND	0.65	ND
2531	SqCC	1B	0.78	0.44	0.44	0.50	ND	1.33	ND
2378	SqCC	1B	0.51	0.35	0.54	0.27	ND	1.07	ND
2193	SqCC	1B	1.40	0.58	0.38	0.36	ND	0.92	ND
2919	SqCC	1B	0.88	1.03	0.98	0.91	ND	0.84	ND
2005	SqCC	1B	0.68	0.96	1.23	1.07	ND	1.03	ND
6091	SqCC	1	0.56	0.45	0.52	0.53	ND	1.01	ND
6495	SqCC	2A	0.68	1.19	1.04	0.58	ND	1.09	ND
6653	SqCC	2B	0.81	1.37	1.21	0.92	ND	1.00	ND
6864	SqCC	2B	1.23	0.74	1.51	1.95	ND	ND	ND
2922	SqCC	2B	0.75	0.29	0.33	0.37	ND	1.25	ND
2783	SqCC	2B	0.52	0.31	0.27	0.46	ND	0.95	ND
2856	SqCC	2B	0.44	0.26	0.28	0.50	ND	0.84	ND
2313	SqCC	2B	0.79	0.66	1.11	0.81	ND	1.24	ND
309	SqCC	3A	0.61	0.65	0.76	0.92	ND	1.18	ND
3698	SqCC	3A	0.52	0.58	0.56	0.62	ND	0.84	ND
6799	SqCC	3B	0.78	0.46	0.56	0.67	ND	0.95	ND
2652	SqCC	3B	0.52	0.22	0.29	0.33	ND	0.91	ND
6964	SqCC	3	0.63	1.15	1.04	0.84	ND	0.97	ND

Figure 1. *FOXO3* deletions in human NSCLC. A, diagrammatic representation of the human *FOXO3* locus. B, relative locations of the FOXO3 sequences analyzed by qPCR. C, representative qPCR analysis of LAC DNA showing deletions within *FOXO3*. D, summary of qPCR data of *FOXO3* and flanking genes. Values shown are gene doses in tumors relative to normal DNA normalized with either *GAPDH* or *β-ACTIN*. Values are the means of several experiments, which resulted in minimal SD. Black, HD; dark gray, sub-HD DNA loss in the range of 60% to 79% decrease; light gray, sub-HD DNA loss in the range of 40% to 59% decrease; white, no DNA loss.

A_{260}/A_{280} (>1.9) and A_{260}/A_{230} (>1.8). Reverse transcription was performed using SuperScript First-Strand cDNA Synthesis kit (Invitrogen) with 1 μg of starting RNA per sample. A negative control without RNA and a negative control without enzyme were analyzed in parallel.

Real-time quantitative reverse transcription-PCR

FOXO3 expression in lung tissue was assessed using Taqman gene expression assays (Applied Biosystems). Expression levels were normalized to GAPDH content. cDNAs were run in quadruplicate and amplified in a 10 μL reaction

Table 1. *FOXO3a* qPCR primers

Name	Forward	Reverse	Length	Position
FOXO3a set 1	CGGGCAGCCGAGGAAATGTT	TGTTGCTGTCGCCCTTATCCTT	172 bp	n555–727 exon 2
FOXO3a set 2	AGATCTACGAGTGGATGGTGCGTT	AAGCGCACTCCGACGAATCCGAGA	168 bp	n668 exon 2–n86 introns 2–3
FOXO3a set 3	TCTCGGATTCGTCGGAGTGCGCTT	TCCAGCAAATGTACTCCTGTCCGT	207 bp	n86–292 introns 2–3
FOXO3a set 4	TGGATTCAGGCACTGTTTGAGGGA	TGGATACCCAACTGCAGGAAGTCA	281 bp	n768–1049 introns 2–3
FOXO3a set 5	TGACTGATATGGCAGGCACCATGA	TTCTCTTGGATGGTCTGCATGGGA	232 bp	n508–740 exon 3
FOXO3a set 6	AAGTGGAGCTGGACCCGGAGTT	TGCTGTCGCCCTTATCCTTGAAGT	558 bp	n166–724 exon 2
FOXO3a set 7	AAGATGGCAGAGGCACCGGCTT	AAGCGCACTCCGACGAATCCGAGA	710 bp	n142–n86 introns 2–3

Published OnlineFirst July 14, 2010; DOI: 10.1158/0008-5472.CAN-09-4008

containing 5 μL of 2× Taqman Universal PCR Master Mix, 0.5 mL of 20× primer/probe mix, and 25 ng of cDNA. Relative quantification of expression was calculated using the $\Delta\Delta C_t$ method. Briefly, ΔC_t was calculated as the C_t value of the target gene (*FOXO3*) minus the C_t value of the control gene (*GAPDH*). The ΔC_t value was then calculated as the ΔC_t value of the sample minus the ΔC_t value of a calibrator sample, in this case the highest expressing adjacent normal tissue. Relative quantification was then determined with the formula $2^{(-\Delta\Delta Ct)}$. FOXO3 mRNA expression was also analyzed by normalization to three additional control genes: *RPLP0, HPRT1*, and *PES1*. These genes were found to be stably expressed in a subset of matched lung tumor and adjacent normal samples (data not shown).

For qPCR data, statistical analyses were done using GraphPad Prism version 5.00. Expression of FOXO3 in matched tumor and adjacent normal tissue was compared using the Wilcoxon signed rank test with significant P value of <0.05. Nonparametric analysis of unpaired samples was analyzed using the Mann-Whitney test with significant P value of <0.05.

Transfections and treatment of cells

Expression vector of FOXO3 cDNA was generated from RNA isolated from human buccal cells. Reverse transcription was carried out on 1 μg of total RNA using 200 units of Moloney murine leukemia virus (MMLV) reverse transcriptase for 1 hour at 37°C. High-fidelity PCR amplification of full-length FOXO3 cDNA used Hi-Fi Platinum Taq DNA polymerase (Invitrogen). Amplified FOXO3 cDNA was cloned into the pCR3.1 mammalian expression vector (Invitrogen), and wild-type clones were confirmed by direct sequence analysis. Transfections of A549 and H358 cells were carried out using Lipofectamine reagent (Invitrogen), with conditions optimized for 1 μg of plasmid DNA in 35-mm^2 dishes. Cells (1×10^5) were seeded into six-well plates (35 mm^2 per well) for transfection. Cells were treated with BPDE (0.4–0.7 μmol/L) for 1 hour following transfection. Twenty-four hours following transfection, cells were plated in selective medium (containing G418). MTS assays were carried out according to the manufacturer's recommendations (Promega) to determine the extent of cell death caused by these treatments. Cells treated with BPDE were also collected at the indicated time points for Western blot analysis, as described below. The pan-caspase inhibitor Z-VAD-FMK (Sigma-Aldrich) was used at a concentration of 15 μmol/L. Treatment with the inhibitor commenced 1 hour before treatment with BPBE.

Reverse transcription-PCR

RNA was isolated using Trizol reagent and subjected to reverse transcription with MMLV reverse transcriptase. PCR was performed on 50 to 100 ng of high-quality cDNA to determine the expression levels of reported FOXO3 effector genes. This was carried out essentially as described above for deletion analysis. Quantitation of target genes was determined by calculating target PCR intensity/control PCR intensity in the test (treated) sample relative to that of the control (untreated) sample. *GAPDH* and *β-ACTIN* were used as control genes for test gene expression quantitation. Quantification was carried out by densitometry using UVP Imaging and Analysis System and LabWorks software. Oligonucleotide primers used in this study were designed based on the available gene sequences from NCBI and Ensembl genome browsers and purchased from Integrated DNA Technologies.

Immunocytochemistry

Formalin-fixed, paraffin-embedded human lung tissue was sectioned at 5 μ and placed on glass slides. A low-temperature antigen retrieval procedure was applied to deparaffinized and rehydrated tissue sections using Antigen Unmasking Solution (Vector Laboratories) at low pH for 1 hour at 80°C. Immunocytochemistry was performed using rabbit monoclonal primary antibody to FOXO3a (Epitomics) diluted 1:50 and incubated overnight at 4°C. The ImmPRESS polymerized reporter enzyme staining system for rabbit antibodies was used (Vector Laboratories). ImmPACT DAB (Vector Laboratories) was used as the chromogen followed by Vector Methyl Green counterstain (Vector Laboratories) or a blush of Eosin Y/Phloxine (Sigma-Aldrich) to visualize cytoplasm. Endogenous peroxidase was inhibited by treating the sections with hydrogen peroxide. Negative control slides were immunostained in the absence of primary antibody. A set of slides matching those stained for FOXO3 was also stained with H&E (Supplementary Fig. S1).

Immunofluorescence

H1299 cells were grown on chamber slides in completed RPMI 1640. At ~50% confluence, the cells were synchronized with 1 mmol/L hydroxyurea in completed medium for 12 hours. Cells were washed twice with culture medium and treated with 0.7 μmol/L BPDE in the same medium for 2, 4, and 8 hours. Cells were fixed with 4% paraformaldehyde for 10 minutes on ice, washed, and permeabilized with PBS/0.02% Triton X-100 and then blocked with PBS/3% bovine serum albumin (BSA). Primary FOXO3 (H-144) and 14-3-3 antibodies were applied to the cells at a concentration of 50 μg/mL and incubated overnight at 4°C. Cy5- and Cy3-conjugated and Cy5 secondary antibodies (Jackson ImmunoResearch Laboratories) were applied following washing at a concentration of 10 μg/mL and incubated at room temperature for 2 hours. Nuclei were stained with Hoechst stain at a dilution of 1:10 for 1 hour at room temperature. Images were acquired with a Leica confocal microscope (TCS SP2 AOBS, Leica Microsystems) using a 488-nm laser for the Cy2, a 543-nm laser for the Cy3, and 633-nm laser for the Cy5 fluorophores. The fluorophores were imaged using a sequential line scan, with detection bands set at 420 to 475 nm for Hoechst stain and 554 to 640 for Cy3. Each image was saved at a resolution of 1,024 × 1,024 pixel image size. The optical sections were reconstructed by maximum projection with the Leica software. This work was done in collaboration with the Microscopy Core Facility at the Pennsylvania State University College of Medicine.

Western blotting

Typically, 25 to 40 μg of whole-cell lysates were denatured in 1× Laemmli sample buffer, electrophoresed, and transferred

Published OnlineFirst July 14, 2010; DOI: 10.1158/0008-5472.CAN-09-4008

onto nitrocellulose membranes. Membranes were blocked with either 5% milk or 5% BSA in TBS with 0.05% Tween 20 for 2 hours. Incubations with primary antibodies were for 2 hours at 4°C, and with secondary antibodies for 45 minutes at room temperature. Antibodies were diluted in 5% milk or 5% BSA in TBS. Rabbit polyclonal anti-FOXO3 (H-144) was used at a dilution of 1:200 (Santa Cruz Biotechnology). Mouse monoclonal anti–β-actin antibody was used at a dilution of 1:3,000 (Sigma-Aldrich). Antibodies used and their sources and concentrations were as follows: mouse monoclonal anti–caspase-7, anti–caspase-8, and anti–caspase-9 were used at dilutions of 1:500 (Stressgen). Rabbit polyclonal anti–α-tubulin was used at a dilution of 1:500 (Santa Cruz Biotechnology). Secondary antibodies were conjugated with horseradish peroxidase and detected by chemiluminescence (Pierce).

Results

FOXO3 is frequently deleted in human LAC

HD of *FOXO3* was detected in 8 of 33 (24.2%) LAC but in none of the LSqCC examined (Fig. 1). Sub-HD was detected in 20 of 33 (60.6%) primary LAC and in 9 of 19 (47.4%) LSqCC (Table 2). The use of several primers within *FOXO3* enabled the identification of exon 2 as the primary site of deletion in the tumors examined (Fig. 1C and D). Most deletions included *FOXO3* primer sets 1 to 4, which span an area of 1,238 bp in exon 2 and extend into intron 2 (Fig. 1B and D; Table 1). Primer sets 6 and 7, which encompass sets 1 to 3, were used to confirm deletions affecting exon 2 (data not shown). Of note, the qPCR analysis was of synonymous or homozygous DNA, which could identify loss of heterozygosity (LOH).

The nearest flanking genes of *FOXO3* were also analyzed for deletion to define more specifically the focus of the observed deletions. Although sub-HDs affected these genes (*ARMC2* and *LACE1*) at a high frequency, none of the HDs of *FOXO3* extended into either gene (Fig. 1D). Similar results are shown for the sub-HD losses of *FOXO3* in the LSqCC. These results identify *FOXO3* as a target of deletion in these tumors.

The *FOXO3* coding region (exons 2 and 3) was also examined by direct sequence analysis for intragenic mutations in several of the LAC and LSqCC. This alternative mechanism of gene inactivation was not detected in any of the tumors examined. Other mechanisms of gene inactivation in cancer were not addressed in this study.

Evidence in mice suggests that *Foxos* may act redundantly as suppressors of some cancer types (35). Therefore, as potential additional targets of selective gene loss in NSCLC, we examined other members of the FOXO gene family by qPCR analysis. We observed that, unlike *FOXO3*, neither *FOXO1* nor *FOXO4* was deleted in any of the tumors of this study (data not shown).

Decreased FOXO3 mRNA expression in LAC

Real-time reverse transcription-PCR (RT-PCR) was conducted on 17 blindly selected NSCLC, surrounding matched noncancerous tissue, and 10 lung samples of cancer-free donors. Relative expression levels were first measured in normal and adjacent tissue to determine the level of FOXO3 expression in both control sets. Expression of FOXO3 was normalized to GAPDH and was very similar in these two sets of tissues. The mean relative quantitation (RQ) expression values were 0.32 ± 0.08 measured in tumor-free tissue and 0.30 ± 0.06 in adjacent normal tissue (Fig. 2).

Expression was then compared between matched tumor and adjacent normal tissue samples (n = 17). The mean FOXO3 RQ value in the tumor tissue was 0.16 ± 0.02, and there was a trend toward lower FOXO3 expression in tumor tissue compared with matched adjacent normal tissue (P = 0.0829; data not shown). However, when stratified by histology, FOXO3 expression in LAC (n = 11) was found to be significantly lower than expression in matched adjacent normal tissues (P = 0.0292; Fig. 2). The mean RQ values for FOXO3 expression were 0.34 ± 0.08 in adjacent normal tissue and 0.14 ± 0.03 in LAC tissue. FOXO3 expression in LSqCC (n = 5) was not significantly different from matched adjacent normal tissue (P = 0.7150). As described in Materials and Methods, FOXO3 expression was also normalized to three experimentally determined control genes—*HPRT1, PES1*, and *RPLP0*—with similarly significant results obtained (data not shown).

FOXO3 protein loss corresponds with gene deletion in LAC

To further investigate the inactivation of FOXO3 in LAC, a sampling of these tumors and noncancerous lung was analyzed for FOXO3 protein expression by immunocytochemistry. Tumor 6784 is shown to stain strongly positive for FOXO3 (Fig. 3A). This is consistent with the qPCR results showing that tumor 6784 has a full complement of *FOXO3*. Relatively strong nuclear staining of FOXO3 is evident in the noncancerous alveoli (Fig. 3B). In contrast, tumors 6379 and 6498 display evidence of FOXO3 loss, which is consistent with the qPCR results indicating HD of *FOXO3* in these tumors (Fig. 3C and D). Heterogeneous staining of FOXO3 is evident in tumor 2621. Areas of both negative and positive staining of FOXO3 were observed on the same slide obtained from this sample (Fig. 3E). This is also consistent with the

Table 2. *FOXO3a* deletion frequency in NSCLC

Tumor	HD	Sub-HD	Total deletion
Adenocarcinoma	8/33 (24.2%)	20/33 (60.6%)	28/33 (84.8%)
Squamous cell carcinoma	0/19	9/19 (47.4%)	9/19 (47.4%)

Published OnlineFirst July 14, 2010; DOI: 10.1158/0008-5472.CAN-09-4008

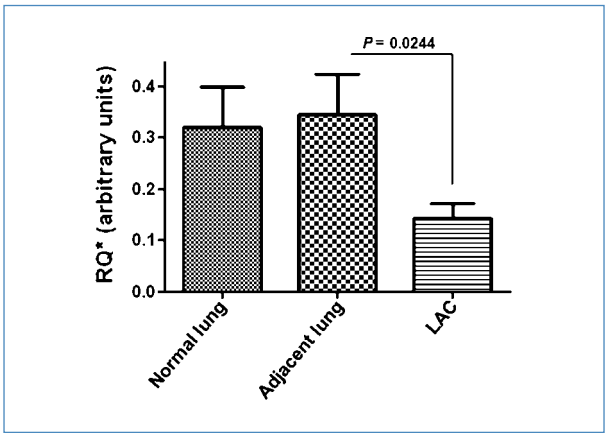

Figure 2. Decreased mRNA expression of FOXO3 in LAC. Real-time RT-PCR shows a significant decrease in FOXO3 mRNA in LAC relative to adjacent noncancer lung tissue and lung tissue of noncancer donors. ANOVA was used to statistically compare the groups of tissues.

qPCR evidence of subclonal deletion of *FOXO3* in this tumor sample. H&E-stained sections of these tumors are shown in Supplementary Fig. S1.

FOXO3 is transcriptionally activated in cells exposed to BPDE

FOXO3 loss in LAC suggests a role in the suppression of these tumors. As a stress-activated transcription factor, FOXO3 may protect against the tumorigenic effects of carcinogens in the pathogenesis of LAC. BPDE is a carcinogenic metabolite of the polycyclic aromatic hydrocarbon (PAH) benzo[a]pyrene (BaP), which is an environmentally pervasive human lung carcinogen (2–4). We next investigated the functional activation of FOXO3 in cells exposed with BPDE. Using immunofluorescence and confocal microscopy, endogenous FOXO3 was observed to localize from the cytosol to the nucleus, indicating its transcriptional activation within 4 hours of exposure of H1299 cells to 0.7 μmol/L BPDE (Fig. 4A).

The transcriptional activation of FOXO3 in response to BPDE was further investigated by quantitative RT-PCR of a set of FOXO3 effector genes (25–30). For these experiments, FOXO3 expression was restored in A549 cells, which have abnormally low levels of endogenous FOXO3 as a result of gene deletion (25). FOXO3- and empty vector–transfected cells were selected for 3 days with G418 to eliminate cells that failed to transfect. Cells were then treated with 0.7 μmol/L BPDE and harvested 18 hours later. A FOXO3-dependent increase in the expression of GADD45B, BIM, BNIP3, and FASL was observed (Fig. 4B). Each of these FOXO3 effectors has been implicated in FOXO3-mediated stress response involving DNA repair (GADD45) and apoptosis (BIM, BNIP3, and FASL).

FOXO3 stimulates apoptosis in response to BPDE in LAC cells

Two different LAC cell lines expressing low endogenous levels of FOXO3 (A549 and H358) were transfected with FOXO3 or empty vector and selected in G418-containing medium. Under these conditions, wild-type FOXO3 caused a significant decrease in the number of viable cells 1 week following transfection (Fig. 5A). Wild-type FOXO3 is transcriptionally active under these conditions, as we have previously reported, resulting in suppression of cell growth (25). The response to BPDE was investigated by treating the selected cells with increasing concentrations (0, 0.4, or 0.7 μmol/L) of BPDE and harvesting after 18 to 36 hours for cell cycle analysis and after 5 days to determine the effect on relative cell number. Exogenous FOXO3 caused a significant decrease in the relative fraction of surviving cells following exposure to 0.7 μmol/L BPDE (Fig. 5B). In contrast, there was no noticeable FOXO3-dependent change in the cell cycle in response to BPDE (Supplementary Fig. S2). These results suggest that FOXO3 augments the sensitivity of LAC cells to BPDE-induced cytotoxicity.

Because we previously showed that FOXO3 elicited apoptosis in response to NNK-induced DNA damage in LAC cells, we next investigated whether FOXO3 also stimulated apoptosis in response to BPDE (25). Experiments were again carried out as described above, and after 24 hours of exposure to 0.7 μmol/L BPDE, apoptosis was measured by fluorescence-activated cell sorting (FACS) selection and quantitation of Annexin V-phycoerythrin (PE)–stained cells. The results showed a significant increase in apoptosis in FOXO3 compared with control transfectants following BPDE treatment (Fig. 5C and D). This analysis was also conducted on stable FOXO3-expressing clones of A549 cells with similar results (Supplementary Fig. S3). Of note, similar results were obtained from both high and low FOXO3-expressing clones (data not shown). Stable independent clones were isolated by dilution following transfection with FOXO3 and clonal expansion during long-term (several weeks) selection with G418.

The role of caspase activation in BPDE-induced apoptosis was examined next. A marked decrease in BPDE-induced, FOXO3-dependent apoptosis was observed when cells were cotreated with 15 μmol/L Z-VAD-FMK, a pan-caspase inhibitor (Fig. 5E). This indicated that FOXO3-dependent apoptosis involved caspase activation. Direct analysis of several caspases by Western blot showed evidence of increased caspase-9, caspase-8, and caspase-7 cleavage activation in FOXO3 relative to control transfectants following treatment with BPDE. These results, together with the RT-PCR results, suggest that FOXO3 stimulates apoptosis involving both intrinsic (FASL–caspase-8) and extrinsic (caspase-9) caspase-dependent apoptotic pathways in response to BPDE. Similar caspase activation was obtained in both A549 (p53-positive) and H358 (p53-negative) LAC cell lines (Supplementary Fig. S4).

Discussion

The results of this study show that *FOXO3* is a novel target of somatic HD in early-stage LAC. This is supported by RT-PCR and immunocytochemistry results showing concomitant losses of both FOXO3 mRNA and protein in these tumors. Our immunocytochemistry results revealed heterogeneous

Published OnlineFirst July 14, 2010; DOI: 10.1158/0008-5472.CAN-09-4008

loss of FOXO3 in individual stage I LAC. Loss of *FOXO3* in several tumors of this early stage, including heterogeneous loss within individual tumors, suggests that *FOXO3* inactivation may play a selective role in this stage of malignancy.

Our results also suggest that *FOXO3* loss may play a role in early-stage LSqCC. Although LSqCC and LAC are pathogenetically and phenotypically distinct types of NSCLC, they do share some molecular changes, such as *TP53* mutation and loss of the *CDKN2* tumor suppressor gene (reviewed in ref. 5). Our analysis of LSqCC detected a decrease in FOXO3 gene dose of >70% in 26% of the patient samples. Although these losses did not meet our conservative threshold for HD, they nevertheless suggest that *FOXO3* loss is also a selective occurrence in the development of this type of NSCLC. This is tempered, however, by our observation that *FOXO3* expression levels were relatively normal in the LSqCC examined. These results therefore suggest that *FOXO3* loss plays a more significant role in LAC than in LSqCC.

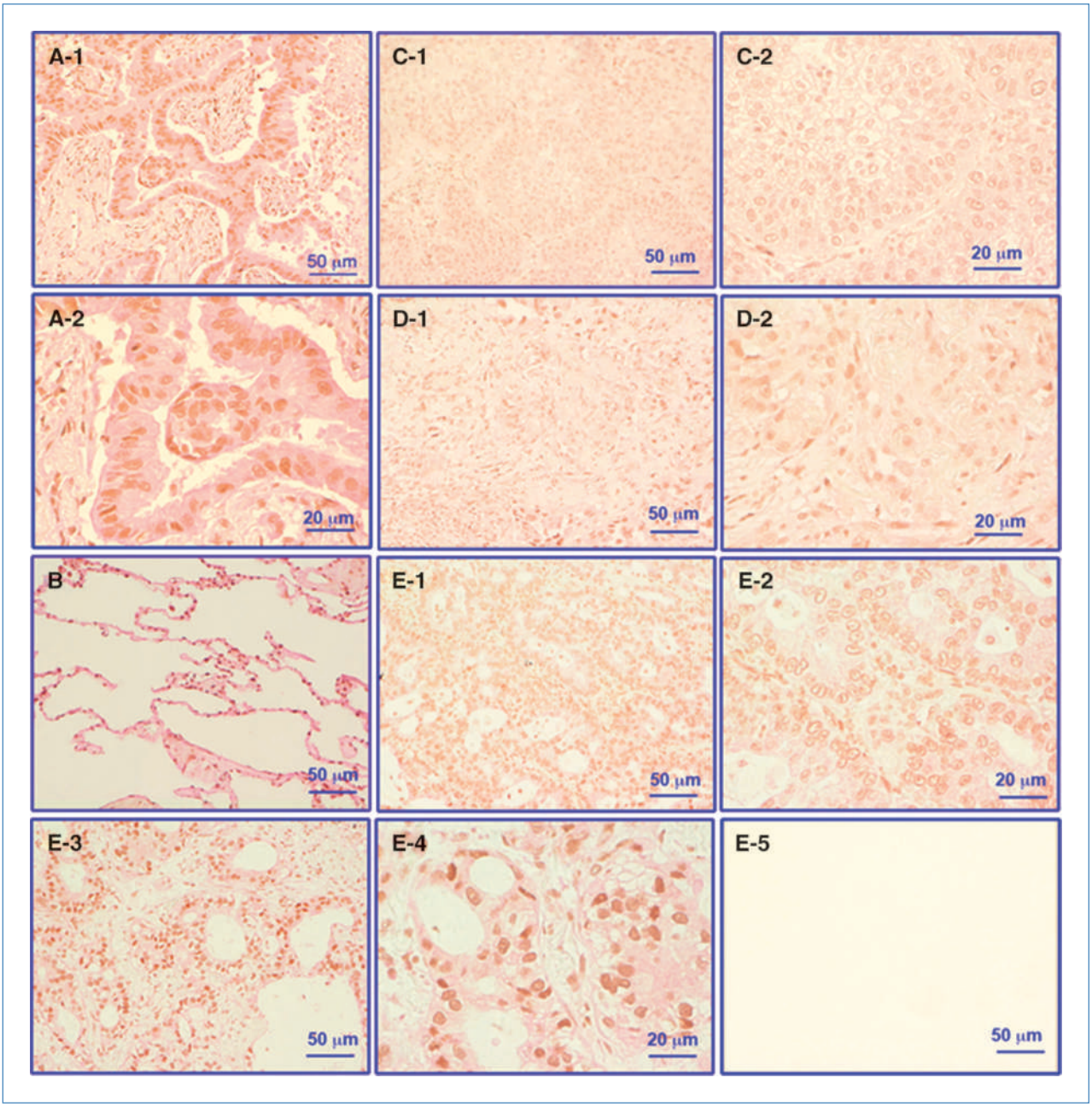

Figure 3. Immunocytochemistry of FOXO3 protein in LAC. A, tumor 6784. B, noncancerous lung alveoli. C, tumor 6379. D, tumor 6498. E, tumor 2621. E-5, negative control lacking primary antibody.

Published OnlineFirst July 14, 2010; DOI: 10.1158/0008-5472.CAN-09-4008

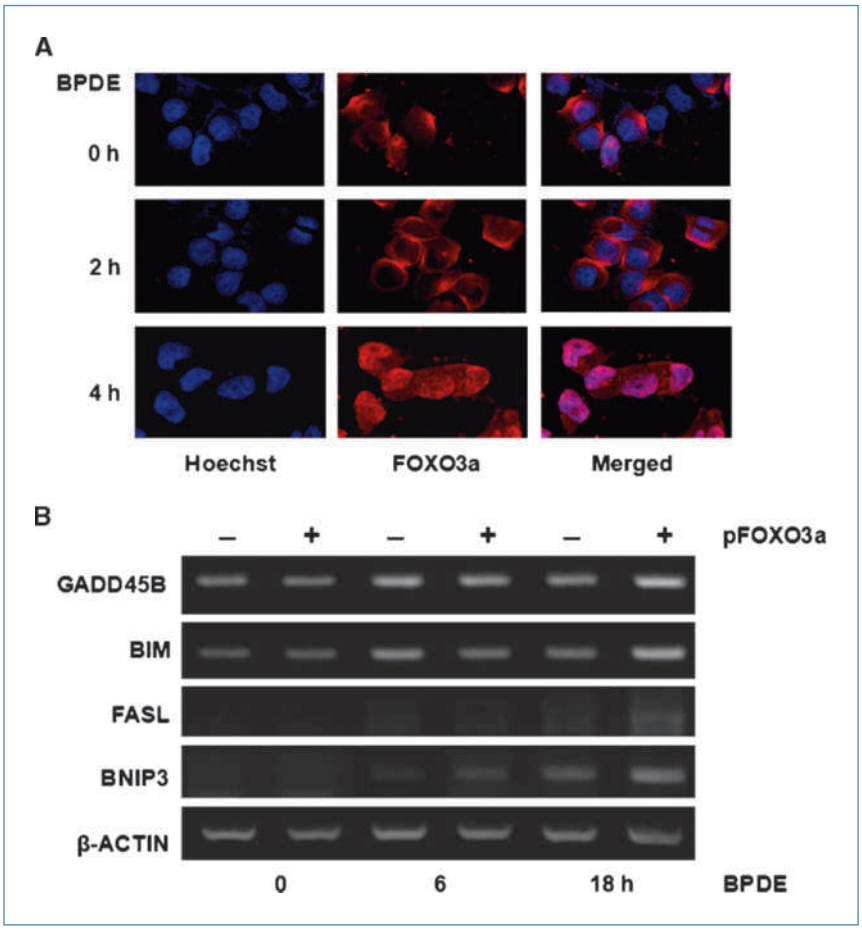

Figure 4. Transcriptional activation of FOXO3 in response to BPDE. A, nuclear localization of endogenous FOXO3 is induced by BPDE in H1299 cells treated with 0.7 μmol/L BPDE for the indicated times. Immunofluorescence was performed as described in Materials and Methods showing localization of FOXO3 to the nucleus 4 h after BPDE exposure. B, representative RT-PCR of FOXO3 effectors in A549 cells transfected with FOXO3 or control vector and treated with 0.7 μmol/L BPDE. Cells were collected at the times shown after treatment for analysis. Results were confirmed by repeat experiments.

In contrast, *FOXO1* and *FOXO4* genes were not deleted in any of the NSCLC examined in this study. *Foxo1, Foxo3*, and *Foxo4* knockout mice have an increased susceptibility for the development of specific cancer types, including thymic lymphomas and hemangiomas. This finding has implicated all of the FOXO genes as tumor suppressors (35). However, the absence of *FOXO1* and *FOXO4* deletions indicates that among these three FOXO genes, *FOXO3* is uniquely targeted for deletion in NSCLC.

Several pieces of evidence suggest that the mechanism of *FOXO3* inactivation in NSCLC may be causally linked with the structure of the *FOXO3* locus and its susceptibility to disruption. Here, we show that *FOXO3* HDs in tumors of smokers are specifically located in a region of the gene lying 5′ to exon 3. It has been reported that active regions of the FRA6F fragile site are located within this part of human *FOXO3* (36). Fragile sites are inherently prone to breakage and consequently are sensitive to DNA-damaging agents, such as genotoxic carcinogens (37, 38). FRA6F has been implicated as a cause of DNA losses at its location on chromosome 6q22-21 in human cancer (38). LOH at this location also is higher in LAC of smokers compared with those of never smokers (39–41). Interestingly, fragile sits are well conserved among mammals, and the same pattern of *FOXO3* deletion was observed in mouse LAC, occurring predominantly in tumors induced by carcinogens (24). The structure of the *FOXO3* locus may therefore be prone to carcinogen-induced disruption, resulting in the occurrence of relatively precisely positioned *FOXO3* HDs in LAC.

An underlying cause of lung cancer is exposure to PAHs such as BaP, which are among the most environmentally pervasive human lung carcinogens (2). Also a component of cigarette smoke, BaP is metabolically activated by cytochrome P450s to BPDE, a highly DNA-reactive and mutagenic diol epoxide (2, 4). Whereas the effects of such DNA-damaging carcinogens are most noticeable in tumor initiation, their effects continue with exposure throughout tumor development. Consequently, carcinogens, such as PAHs, can exert genotoxic stress at any point in tumor development. Taking this into account, we examined the response of FOXO3 to BPDE by restoring its function in LAC cells that apparently had selectively lost *FOXO3* through gene deletion during tumor development. We show that FOXO3 is functionally activated as a transcription factor in LAC cells treated with BPDE, and this activation leads to caspase-dependent apoptosis. In this response, we observed upregulation of three known proapoptotic FOXO3 effector genes: *FASL, BIM*, and *BNIP3*. We previously reported similar results in LAC cells exposed to

Published OnlineFirst July 14, 2010; DOI: 10.1158/0008-5472.CAN-09-4008

a DNA-reactive metabolite of NNK, also a human lung carcinogen present in tobacco smoke (25). Thus, FOXO3 increases the sensitivity of LAC cells to the effects of genotoxic lung carcinogens. The stimulation of apoptosis in these cells suggests a role in eliminating carcinogen-damaged cells as a means of suppressing LAC. The loss of this function may then increase the likelihood that LAC will result from carcinogen exposure.

We previously showed that bulky DNA adduct–forming carcinogens (including NNK) induce extensive chromosome instability (CIN) as a causal mechanism in LAC of mice (42, 43). BPDE also forms bulky DNA adducts but was not investigated in these studies. CIN is a characteristic of most cancers (18, 19). It is an increase in the rate of chromosomal defects that is considered to be a necessary source of genetic variation acted on by selection pressures in the development of most sporadic cancers (18, 19). The loss of "caretaker" functions, which protect the genome from damage, has been shown to underlie CIN in cancer (44, 45). Based on our findings, FOXO3 may act as a caretaker whose loss can enable CIN, causing DNA damage to accumulate or persist. Therefore, FOXO3 loss may also contribute to the emergence of CIN in LAC.

Consistent with this role is evidence that FOXO3 contributes to the repair of damaged DNA. A role in repair of UV-damaged DNA has been associated with its upregulation of

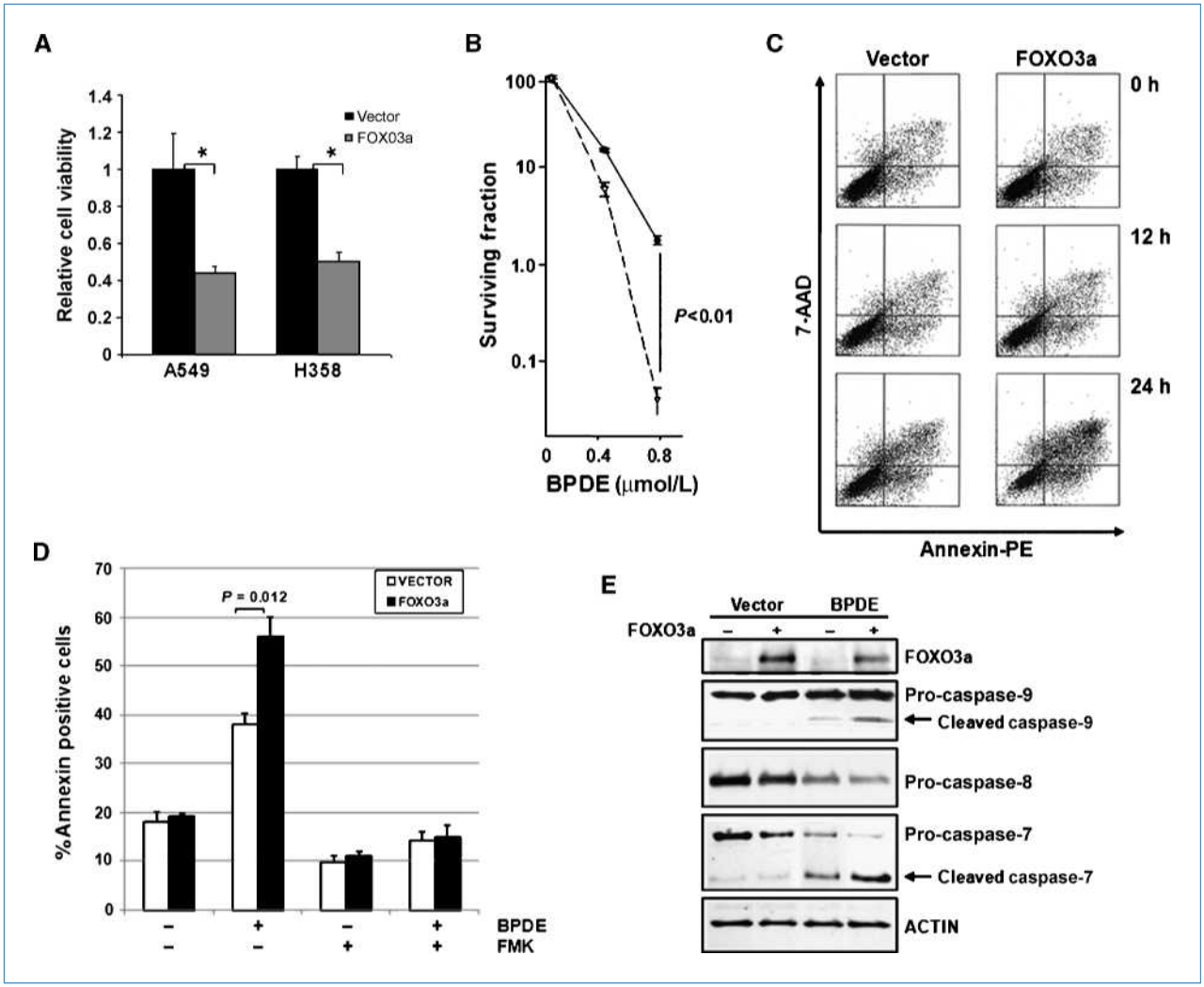

Figure 5. FOXO3 augments apoptosis induced by BPDE in LAC cells. A, MTS assay of A549 and H358 cells following transfection with human wild-type FOXO3 or control vector. Two-tailed Student's *t* test was used to statistically compare the MTS results between FOXO3 and control vector groups. B, MTS assay of transfected A549 cells following treatment with BPDE. Surviving fractions are relative to vehicle (DMSO)–treated cells transfected with the same vector. Black circles, vector transfected; white triangles, FOXO3 transfected. Statistical analysis used was two-tailed Student's *t* test. C, representative FACS analysis selecting for Annexin-PE and 7-aminoactinomycin D (7-AAD) in FOXO3- and control vector–transfected cells treated with 0.7 μmol/L BPDE. Cells were collected for analysis at the times shown following BPDE administration. D, quantitation of Annexin-PE–positive cells following treatment with 0.7 μmol/L BPDE and 15 μmol/L Z-VAD-FMK. E, Western blot of caspases in A549 cells transfected with either FOXO3 or control vector. For Western blot, cells were harvested 12 h after treatment with 0.7 μmol/L BPDE. Results are representative of several experiments.

Published OnlineFirst July 14, 2010; DOI: 10.1158/0008-5472.CAN-09-4008

GADD45 (27). We have shown that GADD45 is also upregulated by FOXO3 in response to NNK-damaged (25) and BaP-damaged DNA (Fig. 4). Repair of DNA damage caused by lung carcinogens may be another means by which FOXO3 suppresses LAC and possibly protects against CIN induction.

On stress activation, FOXO function overrides its negative control by EGFR/PI3K/Akt, resulting in growth arrest or apoptosis. Abnormalities of the EGFR signaling network drive the oncogenesis of LAC and, to a lesser extent, LSqCC (5–10). For example, numerous components of this network have been implicated in LAC, including *EGFR* and *K-ras* mutations and Akt overexpression (5–10, 46). FOXOs are immediately downstream of Akt and are directly negatively regulated by Akt under physiologic conditions suitable for growth and proliferation (26, 34). However, stress activation of FOXOs overrides the prosurvival and oncogenic signaling of Akt, resulting in cell cycle arrest or apoptosis (25–34). The frequent deletion of *FOXO3* therefore would permit unchecked EGFR/PI3K/Akt signaling in the face of DNA damage, arguably conferring a selective advantage for LAC development.

Disclosure of Potential Conflicts of Interest

No potential conflicts of interest were disclosed.

Acknowledgments

We thank D. Shearer and R. Bruggemann for immunocytochemistry and imaging, Dr. A. Barber for confocal microscopy training, and N. Sheaffer and Dr. D. Stanford for assistance with FACS analysis. We are grateful to the Banner Sun Health Research Institute Brain and Body Donation Program of Sun City, Arizona, for the provision of human biological materials (or specific description, e.g., brain tissue and cerebrospinal fluid). The Brain and Body Donation Program is supported by the National Institute on Aging (P30 AG19610 Arizona Alzheimer's Disease Core Center), the Arizona Department of Health Services (contract 211002, Arizona Alzheimer's Research Center), the Arizona Biomedical Research Commission (contracts 4001, 0011, 05-901, and 1001 to the Arizona Parkinson's Disease Consortium), and the Prescott Family Initiative of the Michael J. Fox Foundation for Parkinson's Research.

Grant Support

The Joan Scarangello Foundation to Conquer Lung Cancer.

The costs of publication of this article were defrayed in part by the payment of page charges. This article must therefore be hereby marked *advertisement* in accordance with 18 U.S.C. Section 1734 solely to indicate this fact.

Received 11/02/2009; revised 05/05/2010; accepted 05/27/2010; published OnlineFirst 07/14/2010.

References

1. American Cancer Society. Cancer facts and figures 2008. Atlanta (GA): American Cancer Society; 2008.
2. International Agency for Research on Cancer. Tobacco smoke and involuntary smoking. IARC Monographs on the Evaluation of Carcinogenic Risks to Humans, vol. 83. pp. 35–102Lyon: IARC; 2004.
3. Hecht SS. Tobacco carcinogens, their biomarkers and tobacco-induced cancer. Nat Rev Cancer 2003;3:733–44.
4. Dipple A. DNA adducts of chemical carcinogens. Carcinogenesis 1995;16:437–41.
5. Sekido Y, Fong KM, Minna JD. Molecular genetics of lung cancer. Ann Rev Med 2003;54:73–87.
6. Wistuba II, Mao L, Gazdar AF. Smoking molecular damage in bronchial epithelium. Oncogene 2002;21:7298–306.
7. Sun S, Schiller JH, Gadzar AF. Lung cancer in never smokers—a different disease. Nat Rev Cancer 2007;7:778–90.
8. Ahrendt SA, Decker PA, Alawi EA, et al. Cigarette smoking is strongly associated with mutation of the K-ras gene in patients with primary adenocarcinoma of the lung. Cancer 2001;92:1525–30.
9. Pao W, Wang TY, Riely GJ, et al. KRAS mutations and primary resistance of lung adenocarcinomas to gefitinib or erlotinib. PLoS Med 2005;2:57–61.
10. Paez JG, Jänne PA, Lee JC, et al. EGFR mutations in lung cancer: correlation with clinical response to gefitinib therapy. Science 2004;304:1497–500.
11. Virmani AK, Fong KM, Kodagoda D, et al. Allelotyping demonstrates common and distinct patterns of chromosomal loss in human lung cancer types. Genes Chromosomes Cancer 1998;21:308–19.
12. Petersen I, Bujard M, Petersen S, et al. Patterns of chromosomal imbalances in adenocarcinoma and squamous cell carcinoma of the lung. Cancer Res 1997;57:2331–5.
13. Goeze A, Schlüns K, Wolf G, Thäsler Z, Petersen S, Petersen I. Chromosomal imbalances of primary and metastatic lung adenocarcinomas. J Pathol 2002;196:8–16.
14. Weir BA, Woo MS, Getz G, et al. Characterizing the cancer genome in lung adenocarcinoma. Nature 2007;450:893–8.
15. Chitale D, Gong Y, Taylor BS, et al. An integrated genomic analysis of lung cancer reveals loss of DUSP4 in EGFR-mutant tumors. Oncogene 2009;28:2773–83.
16. Macleod K. Tumor suppressor genes. Curr Opin Genet Dev 2000;10:81–9.
17. Weinberg RA. Prospects for cancer genetics. Cancer Surv 1995;25:3–12.
18. Lengauer C, Kinzler KW, Vogelstein B. Genetic instabilities in human cancers. Nature 1998;396:643–9.
19. Loeb LA. Cancer cells exhibit a mutator phenotype. Adv Cancer Res 1998;72:25–56.
20. Herzog CR, Wiseman RW, You M. Deletion mapping of a putative tumor suppressor gene on chromosome 4 in mouse lung tumors. Cancer Res 1994;54:4007–10.
21. Cairns P, Polascik Y, Eby K. Frequency of homozygous deletion at p16/CDKN2 in primary human tumours. Nat Genet 1995;11:210–2.
22. Loda M. Polymerase chain reaction-based methods for the detection of mutations in oncogenes and tumor suppressor genes. Hum Pathol 1994;25:564–71.
23. Jung R, Soondrum K, Neumaier M. Quantitative PCR. Clin Chem Lab Med 2000;38:833–6.
24. Herzog CR, Blake DC, Jr., Mikse OR, Grigoryiva LS, Gundermann EL. *FOXO3* gene is a target of deletion in mouse lung adenocarcinoma. Oncol Rep 2009;22:837–43.
25. Blake DC, Jr., Mikse OR, Freeman WM, Herzog CR. FOXO3 stimulates a pro-apoptotic transcriptional program in response to human lung carcinogen nicotine-derived nitrosaminoketone. Lung Cancer 2010;67:37–47.
26. Greer EL, Brunet A. FOXO transcription factors at the interface between longevity and tumor suppression. Oncogene 2005;24:7410–25.
27. Tran H, Brunet A, Grenier JM, et al. DNA repair pathway stimulated by the forkhead transcription factor FOXO3 through the Gadd45 protein. Science 2002;296:530–4.
28. Kops GJ, Dansen TB, Polderman PE, et al. Forkhead transcription factor FOXO3 protects quiescent cells from oxidative stress. Nature 2002;419:316–21.
29. Furukawa-Hibi Y, Yoshida-Araki K, Ohta T, Ikeda K, Motoyama N. FOXO forkhead transcription factors induce G(2)-M checkpoint in response to oxidative stress. J Biol Chem 2002;277:26729–32.
30. Bakker WJ, Harris IS, Mak TW. FOXO3 is activated in response to hypoxic stress and inhibits HIF1-induced apoptosis via regulation of CITED2. Mol Cell 2007;28:941–53.
31. Brunet A, Bonni A, Zigmond MJ, et al. Akt promotes cell survival by

Published OnlineFirst July 14, 2010; DOI: 10.1158/0008-5472.CAN-09-4008

phosphorylating and inhibiting a Forkhead transcription factor. Cell 1999;6:857–68.
32. Nakamura N, Ramaswany F, Vasquez S, Signoretti M, Loda M, Sellers WR. Forkhead transcription factors are critical effectors of cell death and cell cycle arrest downstream of PTEN. Mol Cell Biol 2000;20:8969–82.
33. Kops GJ, Medema RH, Glassford J, et al. Control of cell cycle exit and entry by protein kinase B-regulated forkhead transcription factors. Mol Cell Biol 2002;22:2025–36.
34. Daitoku H, Fukamizu A. FOXO transcription factors in the regulatory networks of longevity. J Biochem 2007;141:769–74.
35. Paik JH, Kollipara R, Chu G, et al. FoxOs are lineage-restricted redundant tumor suppressors and regulate endothelial cell homeostasis. Cell 2007;128:309–23.
36. Morelli C, Karayianni E, Magnanini C, et al. Cloning and characterization of the common fragile site FRA6F harboring a replicative senescence gene and frequently deleted in human tumors. Oncogene 2002;21:7266–76.
37. Glover TW, Arl MF, Casper AM, Durkin SG. Mechanisms of common fragile site instability. Hum Mol Genetics 2005;2:197–205.
38. Arlt MF, Durkin SG, Ragland RL, Glover TW. Common fragile sites as targets for chromosome rearrangements. DNA Repair 2006;5:1126–35.
39. Wong MP, Lam WK, Wang E, Chiu SW, Lam CL, Chung LP. Primary adenocarcinomas of the lung in nonsmokers show a distinct pattern of allelic imbalance. Cancer Res 2002;62:4464–8.
40. Sy SM, Wong N, Mok TS, et al. Genetic alterations of lung adenocarcinoma in relation to smoking and ethnicity. Lung Cancer 2003; 41:91–9.
41. Sanchez-Cespedes M, Ahrendt SA, Piantadosi S, et al. Chromosomal alterations in lung adenocarcinoma from smokers and nonsmokers. Cancer Res 2001;61:1309–13.
42. Herzog CR, Bodon N, Pittman B, et al. Carcinogen-specific targeting of chromosome 12 for loss of heterozygosity in mouse lung adenocarcinomas: implications for chromosome instability induction and tumor progression. Oncogene 2004;23:3033–9.
43. Herzog CR, Desai D, Amin S. Array CGH analysis reveals chromosomal aberrations in mouse lung adenocarcinomas induced by the human lung carcinogen 4-(methylnitrosamino)-1-(3-pyridyl)-1-butanone. Biochem Biophys Res Commun 2006;341:856–63.
44. Rajagopalan H, Jallepalli PV, Rago C, et al. Inactivation of hCDC4 can cause chromosomal instability. Nature 2004;428:77–81.
45. Gisselsson D. Chromosome instability in cancer: how, when, and why? Adv Cancer Res 2003;87:1–29.
46. Dutu T, Michiels S, Fouret P, et al. Differential expression of biomarkers in lung adenocarcinoma: a comparative study between smokers and never-smokers. Ann Oncol 2005;16:1906–14.

Cancer Research
The Journal of Cancer Research (1916–1930) | The American Journal of Cancer (1931–1940)

AACR American Association for Cancer Research

FOXO3 Encodes a Carcinogen-Activated Transcription Factor Frequently Deleted in Early-Stage Lung Adenocarcinoma

Oliver R. Mikse, Daniel C. Blake, Jr., Nathan R. Jones, et al.

Cancer Res 2010;70:6205-6215. Published OnlineFirst July 14, 2010.